Neodymium budget in the modern ocean and paleo-oceanographic implications

K Tachikawa, V Athias, C Jeandel

Neodymium budget in the modern ocean and paleo-oceanographic implications

K. Tachikawa,[1] V. Athias, and C. Jeandel

Laboratoire d'Etudes in Géophysique et Océanographie Spatiales, CNES/CNRS/UPS, Observatoire Midi-Pyrénées, Toulouse, France

Received 19 May 1999; revised 7 July 2001; accepted 13 May 2003; published 12 August 2003.

[1] The oceanic Nd budget is calculated using a steady state 10-box model and a compilation of field data. This is the first attempt to propose consistent estimates of the Nd fluxes entering the ocean, as well as indicating possible Nd sources and the proportion of Nd fluxes exchanged between dissolved and particulate fractions. With presently available Nd data the best estimates give a total Nd influx of 9×10^9 g/yr, which leads to an oceanic Nd residence time of 500 years. From modeling tests we suggest that the authigenic Nd scavenged by particulates is 100% remineralized in the deep ocean. The total exchanged Nd flux may be as high as 2×10^{10} g/yr. The $\varepsilon_{Nd(0)}$ values of the influxes are -22, -11, $+1$, and -4 for the North Atlantic, surface Atlantic, North Pacific, and surface Indo-Pacific regions, respectively. Atmospheric and riverine Nd fluxes are insufficient to explain the magnitude and regional variability of calculated Nd influxes and $\varepsilon_{Nd(0)}$. We propose continental margins as an additional source supplying Nd to the ocean. Using the model calibrated for Nd, we examine the sensitivity of deep water $\varepsilon_{Nd(0)}$ to variations of Nd inputs to the ocean. Deep water Nd concentrations and $\varepsilon_{Nd(0)}$ vary with the changes in Nd influxes and their $\varepsilon_{Nd(0)}$. As Nd sources to the ocean may change during glacial/interglacial periods, the $\varepsilon_{Nd(0)}$ shifts recorded in ferromanganese nodules and crusts do not necessarily reflect changes in paleoceanic circulation. The effects of continental erosion should be considered in reconstructing patterns of ocean circulation using Nd isotopes. *INDEX TERMS:* 1040 Geochemistry: Isotopic composition/chemistry; 1050 Geochemistry: Marine geochemistry (4835, 4850); 4267 Oceanography: General: Paleoceanography; *KEYWORDS:* neodymium, isotopes, residence time, budget

Citation: Tachikawa, K., V. Athias, and C. Jeandel, Neodymium budget in the modern ocean and paleo-oceanographic implications, *J. Geophys. Res.*, *108*(C8), 3254, doi:10.1029/1999JC000285, 2003.

1. Introduction

[2] In the modern ocean, seawater Nd isotopic ratio ($^{143}Nd/^{144}Nd$) varies according to the water masses (Figure 1). Since Nd isotopic signatures are preserved in ferromanganese nodules and crusts [*Albarède and Goldstein*, 1992; *Albarède et al.*, 1997; *Burton et al.*, 1997; *O'Nions et al.*, 1998; *Abouchami et al.*, 1999], foraminiferal tests [*Burton and Vance*, 2000] and Fe-Mn oxide coatings of sediments [*Rutherg et al.*, 2000], Nd isotopes could be used to trace past oceanic circulation patterns. However, the Nd budget in the modern ocean is not yet precisely constrained. Before undertaking paleo-oceanographic studies, we need to improve our knowledge of the Nd inventory in the modern ocean.

[3] The $\varepsilon_{Nd(0)}$ values ($\varepsilon_{Nd(0)} = [(^{143}Nd/^{144}Nd)_{sample}/(^{143}Nd/^{144}Nd)_{reference} - 1] \times 10^4$) of the major water masses range from -26 to 0 (Figure 1). Principal Nd sources to the ocean are expected to be continental materials because the flux from the depleted mantle (hydrothermal Nd flux) is negligible [*Elderfield*, 1988, and references therein]. Negative values of $\varepsilon_{Nd(0)}$ in seawater imply the contribution of ancient continental materials to the ocean, whereas values close to zero imply the contribution of young volcanogenic materials [*Faure*, 1986]. Hence the $\varepsilon_{Nd(0)}$ gradient between the North Atlantic ($\varepsilon_{Nd(0)} = \sim -13$) and the North Pacific ($\varepsilon_{Nd(0)} = \sim -4$) is qualitatively explained by the age of the continents surrounding the ocean basins: the North Atlantic is encompassed by old cratonic continents such as Greenland ($\varepsilon_{Nd(0)} = \sim -19$) and the Canadian shield ($\varepsilon_{Nd(0)} = \sim -14/-32$) whereas the North Pacific is surrounded by volcanic rocks such as Japan ($\varepsilon_{Nd(0)} = \sim 0$) and Indonesia ($\varepsilon_{Nd(0)} = \sim +2$) [*Goldstein and Jacobsen*, 1987; *Grousset et al.*, 1988; *Albarède and Goldstein*, 1992].

[4] Continental Nd enters the ocean in the form of dissolved and particulate material from the atmosphere and rivers [*Goldstein and Jacobsen*, 1987; *Elderfield*, 1988; *Spivack and Wasserburg*, 1988; *Bertram and Elderfield*, 1993; *Greaves et al.*, 1994; *Henry et al.*, 1994; *Jeandel et al.*, 1995]. To date, net Nd fluxes from the continents are not precisely quantified. This is partly due to the fact that (i) the net removal of dissolved riverine Nd in estuaries is poorly constrained [*Goldstein and Jacobsen*, 1987; *Elderfield et al.*, 1990; *Sholkovitz*, 1993; *Byrne and Sholkovitz*, 1996] and (ii)

[1] Now at Centre Européen de Recherche et d'Enseignement de Géosciences de l'Environnement, Aix en Provence, France.

0148-0227/03/1999JC000285

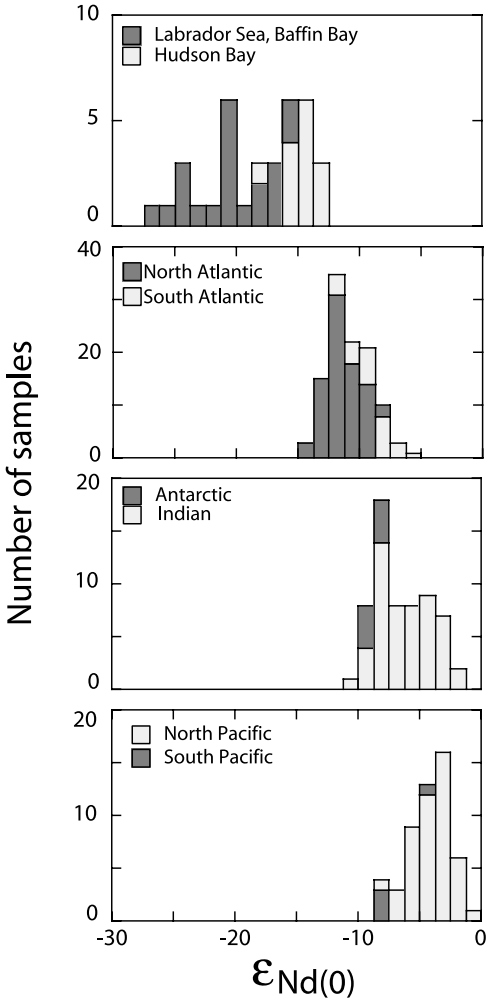

Figure 1. Histogram of seawater $\varepsilon_{Nd(0)}$ of the world ocean. $\varepsilon_{Nd(0)} = [(^{143}Nd/^{144}Nd)_{sample}/(^{143}Nd/^{144}Nd)_{reference} - 1] \times 10^4$, where the reference is (Chondritic Uniform Reservoir (CHUR) representing the bulk earth $\varepsilon_{Nd(0)}$ [*Wasserburg et al.*, 1981]. Data are from *Piepgras et al.* [1979], *Piepgras and Wasserburg* [1980, 1982, 1983, 1987], *Stordal and Wasserburg* [1986], *Piepgras and Jacobsen* [1988], *Spivack and Wasserburg* [1988], *Bertram and Elderfield* [1993], *Jeandel* [1993], *Shimizu et al.* [1994], *Jeandel et al.* [1998], and *Tachikawa et al.* [1999].

the proportions of soluble Nd in atmospheric and riverine particles are highly variable. The net Nd flux from lithogenic (aluminosilicate) particles is the product of the bulk Nd flux and the proportion of soluble Nd. The estimated proportion of soluble Nd in dust varies from 2% to 50% [*Greaves et al.*, 1994; *Henry et al.*, 1994; *Jeandel et al.*, 1995; *Tachikawa et al.*, 1999].

[5] In the ocean, Nd is transported by water masses and marine particles. Dissolved Nd is removed from the surface water by adsorption onto marine particles (scavenging). In deeper waters, the scavenged authigenic Nd is released back to seawater (remineralization). We define the formation of authigenic particulate Nd and its subsequent remineralization as a "dissolved/particulate exchange". The seawater $\varepsilon_{Nd(0)}$ is therefore determined by the mixing of water masses and the dissolved/particulate exchanges. *Bertram and Elderfield* [1993] concluded that an exchanged Nd flux of 4.2×10^{10} g/yr is required to reproduce the distinct $\varepsilon_{Nd(0)}$ observed in the deep Atlantic ($\varepsilon_{Nd(0)} = \sim -13$), Indian ($\varepsilon_{Nd(0)} = \sim -8$) and Pacific ($\varepsilon_{Nd(0)} = \sim -4$). This estimate only holds for the Nd inventory in deep water. It is now necessary to establish a Nd inventory for the whole ocean, including the surface water. Indeed, continental Nd fluxes directly contribute to the surface water and determine the mean oceanic Nd residence time.

[6] The purpose of this study is to constrain the Nd inventory in the modern ocean using both a compilation of all the available Nd data and a numerical model [*Broecker and Peng*, 1987]. We propose to estimate the Nd fluxes from the continents (influxes), the $\varepsilon_{Nd(0)}$ values of theses influxes, the mean Nd residence time and the influence of the dissolved/particulate Nd exchanges. During the last two decades, there has been a remarkable increase in the amount of data on dissolved Nd concentrations and $\varepsilon_{Nd(0)}$. In this study, we use a compilation of Nd data to characterize the 10 boxes of the model [*Broecker and Peng*, 1987] and to improve constraints on the present-day situation of the ocean. The Nd inventory is then calculated using the box model. Finally, the model is calibrated for Nd and used to simulate the effects on deep water $\varepsilon_{Nd(0)}$ of varying Nd inputs to the ocean. To date, changes in deep water $\varepsilon_{Nd(0)}$ recorded in ferromanganese nodules and crusts have been explained in terms of changes in deep water circulation. However, it is well known that lithogenic element fluxes and sources to the ocean vary during glacial/interglacial periods because of several factors such as wind strength, aridity of continents and erosion by ice sheets [*Williams et al.*, 1998]. Our results suggest that deep water $\varepsilon_{Nd(0)}$ may change in response to Nd inputs, even though the circulation pattern remains unchanged.

2. Modeling

2.1. General Assumptions

[7] In the PANDORA model [*Broecker and Peng*, 1987], the ocean is described by 10 boxes whose volumes and surface areas are known (Figure 2a and Table 1). Each box is characterized by a dissolved Nd concentration, a dissolved $\varepsilon_{Nd(0)}$, as well as dissolved and particulate Nd fluxes entering and leaving the box. Except for the North Pacific (box 7), the Indian and Pacific boxes are combined and referred as to INDOPAC boxes. The INDOPAC boxes are assumed to be composed of 70% of the Pacific Ocean and 30% of the Indian Ocean. Six hypotheses are applied to the Nd modeling.

[8] 1. Neodymium is thought to be at steady state in the modern ocean. This implies, first, that the total amount of Nd in each box i is constant with time, because the influxes are balanced by the outfluxes:

$$\frac{dQ_i}{dt} = V_i \frac{dC_i}{dt} = \sum_{j \neq i} F_{j \to i} - \sum_{j \neq i} F_{i \to j} = 0 \qquad (1)$$

where $F_{j \to i}$ indicates the Nd flux entering box i from box j, and $F_{i \to j}$ indicates the Nd flux leaving box i to box j. Q_i is the total amount of Nd in box i. V_i and C_i are the volume and the dissolved Nd concentration of box i, respectively. We define the total amount of Nd contained in each box as follows: $Q_i = V_i C_i$.

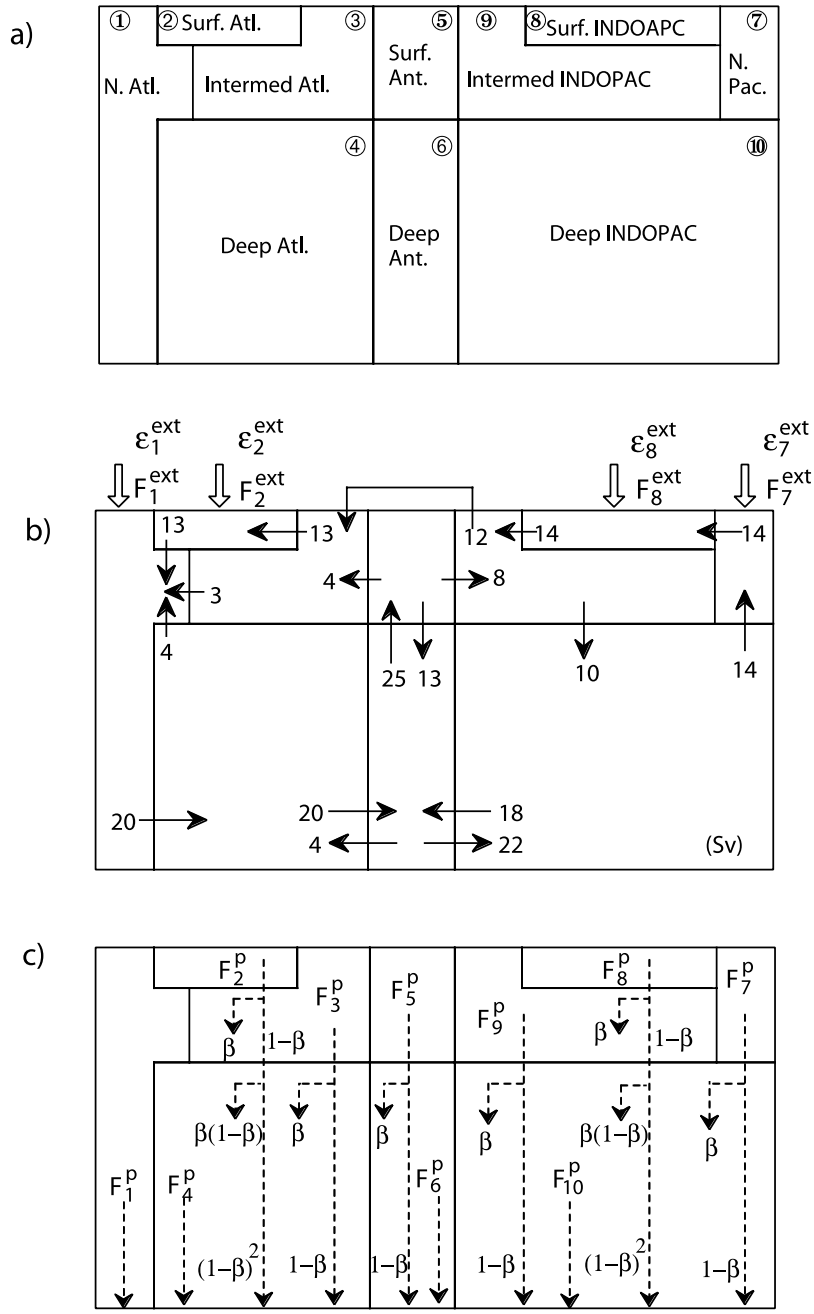

Figure 2. PANDORA 10-box model [*Broecker and Peng*, 1987]. (a) Configuration of the model. Atl., Atlantic; Ant., Antarctic; Pac., Pacific; INDOPAC, Indian and Pacific; Surf., Surface; Intermed., Intermediate; and N, North. (b) Water fluxes (solid arrows) were calibrated by *Broecker and Peng* [1987] (Sv, Sverdrups = 10^6 m^3/s). Four open arrows toward surface boxes indicate the Nd fluxes entering the ocean (Table 3). (c) Remineralization pattern of the particulate Nd fluxes. Remineralization rate is denoted as β. Note that our remineralization pattern is different from the original version [*Broecker and Peng*, 1987] for the North Atlantic box. There is no contribution of remineralized particulate flux from the Surface Atlantic to the North Atlantic box. This is necessary to avoid forming a negative flux in the North Atlantic box.

[9] The steady state hypothesis also means that the $\varepsilon_{Nd(0)}$ of box i (ε_i) does not change with time:

$$\frac{d\varepsilon_i}{dt} = \frac{1}{Q_i}\left[\sum_{j\neq i} F_{j\rightarrow i}\cdot\varepsilon_j - \sum_{j\neq i} F_{i\rightarrow j}\cdot\varepsilon_i\right] = 0 \qquad (2)$$

Hence ε_i is determined by the influxes entering box i as well as the $\varepsilon_{Nd(0)}$ values of the influxes:

$$\varepsilon_i = \frac{\sum_{j\neq i} F_{j\rightarrow i}\cdot\varepsilon_j}{\sum_{j\neq i} F_{j\rightarrow i}} \qquad (3)$$

Table 1. Nd Concentrations and Isotopic Ratios for the 10 PANDORA Boxes

Box				Field Data		Values Applied to the Model	
No.	Name	Volume, 10^{16} m^3	Area,[a] 10^{13} m^2	Nd, pmol/kg	$\varepsilon_{Nd(0)}$	Nd, pmol/kg C_i	$\varepsilon_{Nd\ (0)}$ ε_i
1	North Atlantic (>50°N)	8.2	1.1	20.8 ± 4.7 (124)	−13.9 ± 3.8 (21)	20.8	−13.9
2	Surface Atlantic	4.1	10.1	14.9 ± 5.9 (47)	−11.2 ± 1.1 (30)	14.9	−11.2
3	Intermediate Atlantic	4.1	1.4 10.5	13.8 ± 5.6 (40)	−10.1 ± 1.8 (23)	13.8	−10.1
4	Deep Atlantic	26.1	11.6	21.4 ± 8.0 (76)	−11.1 ± 2.1 (44)	21.4	−11.1
5	Surface Antarctic	1.4	1.4	11.6 ± 3.6 (4)	−9.1 ± 0.1 (3)	11.6	−8.2
6	Deep Antarctic	13.7	1.4	21.7 ± 7.9 (3)	−8.5 ± 0.4 (3)	21.7	−8.2
7	North Pacific (> 44°N)	1.4	1.1	22.1 ± 3.7 (5)	−4.0 ± 2.5 (6)	22.1	−4.0
8	Surface INDOPAC	8.3	19.5	8.2 ± 3.2 (151)	−4.3 ± 2.3 (43)	8.2	−4.3
9	Intermediate INDOPAC	16.5	1.4 20.9	14.0 ± 5.1 (52)	−4.6 ± 1.7 (26)	14.0	−4.6
10	Deep INDOPAC	53.5	22.0	26.9 ± 10.5 (107)	−5.6 ± 2.1 (64)	26.9	−5.6
	Whole ocean	137	36.1	4.2 × 10^{12}(g)		4.2 × 10^{12}(g)	

Numbers between the blankets indicate numbers of data.

[a]For two intermediate boxes (boxes 3 and 9), both surface and bottom areas are indicated (Figure 2a).

[b]The mean Nd concentration and ε_{Nd} as well as their 2σ are calculated from the data [*Piepgras et al.*, 1979; *Piepgras et al.,* 1982, 1983, 1987; *Elderfield and Greaves*, 1982; *De Baar et al.*, 1985, 1988; *Stordal and Wasserburg*, 1986; *Spivack and Wasserburg*, 1988; *German and Elderfield*, 1989, 1990; *Greaves et al.*, 1991; *Sholkovitz and Schneider*, 1991; *Westerlund and Ohman*, 1992; *Jeandel*, 1993; *Bertram and Elderfield*, 1993; *Zhang et al.*, 1994; *Nozaki and Zhang*, 1995; *German et al.*, 1995; *Zhang and Nozaki*, 1996; *Jeandel et al.*, 1998; *Tachikawa et al.*, 1999; *Amakawa et al.*, 2000; *Lacan and Jeandel*, 2001].

[10] 2. The continental Nd is assumed to enter the ocean via four surface boxes in the northern hemisphere: North Atlantic (i = 1), Surface Atlantic (i = 2), North Pacific (i = 7) and Surface INDOPAC (i = 8) (Figure 2b). The fluxes to the Southern Ocean are assumed to be negligible because of the long distances from the continents.

[11] Under this hypothesis, equation (1) for the four surface boxes (i = 1, 2, 7, 8) becomes as follows:

$$V_i \frac{dC_i}{dt} = \left(F_i^{ext} + \sum_{j \neq i} F_{j \to i}^{ad} \right) - \left(\sum_{j \neq i} F_{i \to j}^{ad} + F_i^p \right) = 0 \qquad (4)$$

where F_i^{ext} is the Nd flux from external sources toward box i and F_i^p is the authigenic particulate Nd flux formed in box i. $\Sigma F_{i \to j}^{ad}$ and $\Sigma F_{j \to i}^{ad}$ are the sums of advective Nd fluxes entering and leaving box i, respectively. The advective Nd fluxes $F_{i \to j}^{ad} (1 \leq i \leq 10, 1 \leq j \leq 10, i \neq j)$ are the products of seawater Nd concentration (C_i) and water flux ($F_{i \to j}^{ad,sw}$), that is $F_{i \to j}^{ad} = C_i \cdot F_{i \to j}^{ad,sw}$. All the $F_{i \to j}^{ad,sw}$ values have already been determined from the oceanic ^{14}C distribution by *Broecker and Peng* [1987] (Figure 2b). $F_{i \to j}^{ad,sw}$ values are assumed not to vary with time.

[12] 3. A fixed proportion of Nd present in the authigenic particulate Nd flux is assumed to be remineralized in the deeper boxes in the Atlantic, Indian and Pacific Oceans ($0\% \leq \beta \leq 100\%$). This proportion, denoted here as β, is assumed to be constant with respect to ocean basin, water depth and time.

[13] When β is 0%, no remineralization occurs. When β is 100%, all the particulate authigenic Nd dissolves. The remineralization is schematically presented in Figure 2c. The Intermediate Atlantic, Deep Antarctic and Intermediate INDOPAC (i = 3, 6, 9) receive a remineralized authigenic Nd flux formed in the respective surface box. Hence equation (1) for these boxes (i = 3, 6, 9) is as follows:

$$V_i \frac{dC_i}{dt} = \left(\beta \cdot F_{i-1}^p + \sum_{j \neq i} F_{j \to i}^{ad} \right) - \left(\sum_{j \neq i} F_{i \to j}^{ad} + F_i^p \right) = 0 \qquad (5)$$

The Deep Atlantic and Deep INDOPAC boxes (i = 4, 10) receive remineralized Nd fluxes formed in both surface and intermediate boxes:

$$V_i \frac{dC_i}{dt} = \left(\beta \cdot F_{i-1}^p + \delta_{i,10} \cdot \left(\beta \cdot F_7^p \right) + \beta \cdot (1 - \beta) \cdot F_{i-2}^p + \sum_{j \neq i} F_{j \to i}^{ad} \right) - \left(\sum_{j \neq i} F_{i \to j}^{ad} + F_i^p \right) = 0 \qquad (6)$$

where $\delta_{i,j}$ is a Kronecker symbol defined such that $\delta_{i,j} = 0$ when $i \neq j$ and $\delta_{i,j} = 1$ when i = j.

[14] 4. Dissolved Nd concentrations (C_i) and $\varepsilon_{Nd(0)}$ (ε_i) in the 10 boxes can be determined from field data. Table 1 compiles all the available data on seawater Nd concentrations and $\varepsilon_{Nd(0)}$. The mean Nd concentrations (C_i) were estimated taking into account the different Nd concentrations in the north and south basins. Volume-weighted averages of the north and south basins were used to determine C_i (Table 1). Similarly, seawater $\varepsilon_{Nd(0)}$ values are systematically different between the north and south basins (Figure 1). The mean $\varepsilon_{Nd(0)}$ values (ε_i) were estimated considering both volumes and Nd concentrations of the north and south basins (Table 1). Because of the limited amount of $\varepsilon_{Nd(0)}$ data (n = 3) for the Surface and Deep Antarctic boxes, ε_5 and ε_6 were determined using the $\varepsilon_{Nd(0)}$ equation at steady state (equation (3)). Equation (3) for the surface and deep Antarctic (i = 5, 6) becomes:

$$\varepsilon_5 = \frac{F_{6 \to 5}^{ad} \cdot \varepsilon_6}{F_{6 \to 5}^{ad}} = \varepsilon_6$$

$$\varepsilon_6 = \frac{\varepsilon_4 \cdot F_{4 \to 6}^{ad} + \varepsilon_5 \cdot F_{5 \to 6}^{ad} + \varepsilon_{10} \cdot F_{10 \to 6}^{ad} + \varepsilon_5 \cdot \beta \cdot F_5^p}{F_{4 \to 6}^{ad} + F_{5 \to 6}^{ad} + F_{10 \to 6}^{ad} + \beta \cdot F_5^p} \qquad (7a)$$

or

$$(\varepsilon_6 - \varepsilon_5) \cdot \beta \cdot F_5^p = \left(\varepsilon_4 \cdot F_{4 \to 6}^{ad} + \varepsilon_5 \cdot F_{5 \to 6}^{ad} + \varepsilon_{10} \cdot F_{10 \to 6}^{ad} \right) - \varepsilon_6 \left(F_{4 \to 6}^{ad} + F_{5 \to 6}^{ad} + F_{10 \to 6}^{ad} \right) \qquad (7b)$$

The left-hand side of equation (7b) is zero because $\varepsilon_5 = \varepsilon_6$ (equation (7a)). Consequently, equation (7b) can be rearranged:

$$\varepsilon_5 = \varepsilon_6 = \frac{\varepsilon_4 \cdot F^{ad}_{4\to6} + \varepsilon_{10} \cdot F^{ad}_{10\to6}}{F^{ad}_{4\to6} + F^{ad}_{10\to6}} \quad (7c)$$

Using ε_4, ε_{10}, C_4 and C_{10} shown in Table 1, $\varepsilon_5 = \varepsilon_6 = -8.2$. This value is used for the model calculation.

[15] At present, all the Nd concentrations (C_i) and all the $\varepsilon_{Nd(0)}$ values (ε_i) of the boxes are known. All the advective Nd fluxes ($F^{ad}_{i\to j}$) then become known because both C_i and water fluxes ($F^{ad,sw}_{i\to j}$) can be determined. Under the four hypotheses, the Nd inventory is described by 20 equations: 10 for the $\varepsilon_{Nd(0)}$ values (equation (3)) and 10 for the Nd fluxes (equation (4), (5), or (6), depending upon box number). In this study, we aim to determine 19 unknowns including 4 Nd fluxes from the external sources (F^{ext}_1, F^{ext}_2, F^{ext}_7 and F^{ext}_8), 4 $\varepsilon_{Nd(0)}$ values of the external fluxes (ε^{ext}_1, ε^{ext}_2, ε^{ext}_7 and ε^{ext}_8), 10 authigenic particulate Nd fluxes formed in the boxes (F^p_i) and 1 remineralization rate (β). Among the 20 equations, only 17 effectively need to be considered. First, there are no unknown values in equation (3) for i = 5 ($\varepsilon_5 = \varepsilon_6$) and equation (7c) for i = 6. Second, the two equations shown below express the same relationship between F^p_2, F^p_3 and β:

$$\varepsilon_4 = \frac{\varepsilon_1 \cdot F^{ad}_{1\to4} + \varepsilon_6 \cdot F^{ad}_{6\to4} + \varepsilon_2 \cdot \beta \cdot (1-\beta) \cdot F^p_2 + \varepsilon_3 \cdot \beta \cdot F^p_3}{F^{ad}_{1\to4} + F^{ad}_{6\to4} + \beta \cdot (1-\beta) \cdot F^p_2 + \beta \cdot F^p_3} \quad (8a)$$

$$\left(F^{ad}_{5\to3} + F^{ad}_{9\to3} + \beta \cdot F^p_2\right) - \left(F^{ad}_{3\to1} + F^{ad}_{3\to2} + \beta \cdot F^p_3\right) = 0 \quad (8b)$$

Equation (8a) corresponds to equation (3) for i = 4, whereas equation (8b) is equation (4) for i = 3. To maintain consistency of the system, the expressions relating F^p_2, F^p_3 and β in equations (8a) and (8b) must be identical. This point is examined in section 2.4. In the model calculations, we use equation (8b) for the sake of simplicity. Since the number of unknowns (n = 19) exceeds the number of equations (n = 17), some further hypotheses are required.

[16] 5. The authigenic particulate Nd flux formed in the North Atlantic box (F^p_1) is assumed to be known from the field data. The Nd inventory in the North Atlantic box (i = 1) is described by equation (3) for $\varepsilon_{Nd(0)}$ and equation (4) for Nd fluxes:

$$\varepsilon_1 = \frac{\varepsilon^{ext}_1 \cdot F^{ext}_1 + \varepsilon_2 \cdot F^{ad}_{2\to1} + \varepsilon_3 \cdot F^{ad}_{3\to1} + \varepsilon_4 \cdot F^{ad}_{4\to1}}{F^{ext}_1 + F^{ad}_{2\to1} + F^{ad}_{3\to1} + F^{ad}_{4\to1}} \quad (9)$$

$$\left(F^{ext}_1 + F^{ad}_{2\to1} + F^{ad}_{3\to1} + F^{ad}_{4\to1}\right) - \left(F^{ad}_{1\to4} + F^p_1\right) = 0 \quad (10)$$

As the two equations contain three unknowns (F^{ext}_1, ε^{ext}_1 and F^p_1), we need to assume that one of the three unknowns is already determined. We propose that F^p_1 is known from field data (see section 2.2). To check this hypothesis, we test the sensitivity of F^{ext}_1 and ε^{ext}_1 with respect to F^p_1 (see section 2.3).

[17] 6. To a first approximation, the remineralization rate (β) is assumed to be 100%. This hypothesis is based on the behavior of authigenic ^{230}Th in the water column. The in situ decay of ^{234}U produces ^{230}Th which is scavenged from surface waters because of its high reactivity with marine particles. The interaction between the dissolved and particulate ^{230}Th is considered to be totally reversible [*Bacon and Anderson*, 1982; *Roy-Barman et al.*, 1996]. This implies that β for the authigenic ^{230}Th can attain a value of 100% and that remineralization occurs rapidly. Since authigenic Nd is more labile than authigenic ^{230}Th [*Arraes-Mescoff et al.*, 2001], β for Nd is assumed to be 100%. This hyopothesis is discussed further in section 2.4.

[18] According to the six hypotheses, the Nd inventory in the modern ocean can be described by 17 equations containing 17 unknowns. In the following section, we estimate the scavenged Nd fluxes using field data in order to determine F^p_1 and to compare the modeled Nd fluxes with the field data.

2.2. Authigenic Particulate Nd Fluxes and Scavenged Nd Fluxes

[19] First, we define the relationship between the authigenic particulate Nd fluxes (F^p_i) and scavenged Nd fluxes (F^{scav}_i). For the five surface boxes (North Atlantic, Surface Atlantic, Surface Antarctic, North Pacific and Surface INDOPAC: i = 1, 2, 5, 7, 8), the scavenged flux is equal to the authigenic flux (Figure 2c):

$$F^{scav}_i = F^p_i \quad (11a)$$

For the Intermediate Atlantic (i = 3), Intermediate INDOPAC (i = 9) and Deep Antarctic (i = 6), the scavenged Nd flux is the sum of the remaining authigenic flux from the surface, $(1-\beta)\cdot F^p_{i-1}$, and the particulate flux formed in the box (F^p_i):

$$F^{scav}_i = (1-\beta) \cdot F_{i-1^p} + F^p_i \quad (11b)$$

For the Deep Atlantic and INDOPAC (i = 4, 10), we consider the authigenic fluxes formed in both the surface and intermediate boxes which remain after the remineralization:

$$F^{scav}_i = (1-\beta)^2 \cdot F^p_{i-2} + (1-\beta) \cdot F^p_{i-1} + F^p_i + \delta_{i,10} \cdot (1-\beta) \cdot F^p_7 \quad (11c)$$

[20] Field data on sediment-trapped materials give the range of scavenged Nd fluxes. The bulk trapped material contains both scavenged and lithogenic Nd. We used three methods to distinguish authigenic Nd from lithogenic Nd: model calculation [*Murphy and Dymond*, 1984], chemical leaching [*Tachikawa*, 1997; *Lerche and Nozaki*, 1998] and a subtraction of lithogenic Nd from bulk data using lithogenic Nd/Th or Nd/Al ratios [*Taylor and McLennan*, 1985; *Masuzawa and Koyama*, 1989; *Tachikawa et al.*, 1997; *Fagel et al.*, 1999]. Trap data used in this study come from the OMEX sites in the North Atlantic (49°11′N, 12°49′W; 49°05′N, 13°25′W; 49°02′N, 13°42′W [*Fagel et al.*, 1999]), EUMELI sites in the subtropical Atlantic (18°N, 21°W; 21°N, 31°W [*Tachikawa*, 1997]), the Japan Sea (40°50′N, 138°40′E [*Masuzawa and Koyama*, 1989]), MANOP site H

Table 2. Authigenic Particulate Nd Fluxes and Scavenged Nd Fluxes Calculated From the Model Together With Scavenged Nd Fluxes Estimated From Field Data

	Authigenic Nd flux (g/yr)	Scavenged Nd flux (10^{-5} g/m^2/yr)		
Box	Calculated (β = 100%)	Calculated (β = 100%)	Field data	Reference[b]
1. N. Atl. (>50°N)	*8.6 ×10^7*	*0.79*	0.794 (n = 1)	1
2. Surf. Atl.	4.2 × 10^9	4.16	2.18 ± 1.98 (n = 2)	1, 2
3. Intermed. Atl.	4.2 × 10^9	3.79	15.7 ± 19.2 (n = 3)	1, 2
4. Deep Atl.	4.1 × 10^9	3.55	7.32 ± 8.65 (n = 4)	1, 2
5. Surf. Ant.	1.2 × 10^9	7.97	n.d.	
6. Deep Ant.	9.5 × 10^8	6.59	n.d.	
7. N. Pac. (>44°N)	8.3 × 10^8	7.69	5.28 ± 3.33 (n = 2)[a]	3
8. Surf. INDOPAC	4.2 × 10^9	2.00	2.51 ± 3.44 (n = 2)	3, 4
9. Intermed. INDOPAC	3.7 × 10^9	1.78	5.29 ± 3.85 (n = 6)	3, 4, 5
10. Deep INDOPAC	3.4 × 10^9	1.57	6.99 ± 6.05 (n = 7)	3, 4, 5

n.d. = not determined.
italic = pre-determined from field data (see text for detail).
[a]No data are available in the North Pacific (>44°N). Estimate from data of the Japan Sea (40°N50′; [*Masuzawa and Koyama*, 1989]).
[b]1 = [*Fagel et al.*, 1999] (North Atlantic), 2 = [*Tachikawa*, 1997] (Subtropical Atlantic), 3 = [*Masuzawa and Koyama*, 1989] (Japan Sea), 4 = [*Murphy and Dymond*, 1984] (North Pacific) and 5 = [*Lerche and Nozaki*, 1998] (Japan Trench).

in the equatorial Pacific (6°5′N, 93°W [*Murphy and Dymond*, 1984]) and the Japan Trench (34°01′N, 141°50′E [*Lerche and Nozaki*, 1998]). No direct data are available for the Antarctic boxes (i = 5, 6) or the North Pacific (i = 7).

[21] Using the OMEX result, F_1^p is estimated at 8.6 × 10^7 g/yr (0.78 × 10^{-5} g/m^2/yr). This estimate is used for the model calculation. All the scavenged Nd fluxes estimated from field data are compiled in Table 2.

2.3. Modeled F_i^{ext}, ε_i^{ext}, Oceanic Nd Residence Time, Scavenged Nd Fluxes, and Exchanged Nd Fluxes Assuming β is 100%

[22] The total Nd flux from the external sources toward the ocean ($F_1^{ext} + F_2^{ext} + F_7^{ext} + F_8^{ext}$) is estimated at 8.6 × 10^9 g/yr (Table 3). Using this total Nd influx, the mean Nd residence time (τ_{Nd}) is determined by:

$$\tau_{Nd} = \frac{Q}{F_1^{ext} + F_2^{ext} + F_7^{ext} + F_8^{ext}} \quad (12)$$

Knowing the total amount of Nd in the ocean (Q = 4.2 × 10^{12} g: Table 1), τ_{Nd} is estimated at 487 yr. This value is consistent with the lower limit of previous estimates: 200 ∼ 300 years [*Piepgras and Wasserburg*, 1983] and ∼600 years [*Tachikawa et al.*, 1999]. As mentioned in section 2.1, F_1^{ext} depends on F_1^p, while F_1^p is assumed to be predetermined from field data. Provided that the uncertainty of the predetermined F_1^p does not exceed one order of magnitude, the estimated F_1^{ext} ranges between 4.4 × 10^8 and 1.3 × 10^9 g/yr. This leads to a τ_{Nd} of between 490 and 450 years.

[23] Neodymium sources to the ocean are characterized by ε_i^{ext} values. The calculated ε_1^{ext}, ε_2^{ext}, ε_7^{ext} and ε_8^{ext} are −22.0, −11.4, +1.1, and −4.4, respectively (Table 3). These values are qualitatively consistent with nonradiogenic old materials contributing to the Atlantic and more radiogenic young materials contributing to the Pacific. In the same way as for F_1^{ext}, ε_1^{ext} depends on F_1^p. Using the same uncertainty as with F_1^p, we obtain $\varepsilon_1^{ext} = -20 \pm 3$.

[24] We can now compare the modeled scavenged Nd fluxes (F_i^{scav}) with the estimates from field data (Figure 3 and Table 2). The field data used for the North Pacific box (i = 7) are derived from data in the Japan Sea (40°50′N) because no direct measurements are available in the Pacific north of 44°N. All the calculated F_i^{scav} are in agreement with the field data within error (Figure 3). The calculated F_i^{scav} values are the highest in the surface boxes and decrease toward the respective intermediate and deep boxes (Table 2). This tendency is generally observed in the real ocean.

Table 3. Comparison of the Nd Fluxes (g/yr) and $\varepsilon_{Nd(0)}$ Between the Calculated Influxes and Some Potential Sources

	Calculated influx		"Missing"[a]		Redissolution in estuaries[b]		30% of dust dissolution[c]	
Box	F_i^{ext}	ε_i^{ext}	Flux	$\varepsilon_{Nd(0)}$	Flux	$\varepsilon_{Nd(0)}$	Flux	$\varepsilon_{Nd(0)}$
1. N. Atl.	5.2 · 10^8	−22.0	4 · 10^8	−24	3 · 10^8	−17	3 · 10^7	−15
2. Surf. Atl.	4.3 · 10^9	−11.4	4 · 10^9	−11	6 · 10^8	−11	2 · 10^9	−12
7. N. Pac.	5.3 · 10^8	+1.1	5 · 10^8	+2	4 · 10^7	−6	4 · 10^8	−5
8. Surf. INDOPAC	3.3 · 10^9	−4.4	3 · 10^9	−4	2 · 10^8	−4	3 · 10^9	−7
Global	8.6 · 10^9	−8.6	8 · 10^9	−9	1 · 10^9	−11	6 · 10^9	−8

[a]The difference between the calculated global flux and the sum of dissolved river flux (70% of Nd removal in estuaries) and atmospheric flux (2% of Nd dissolution). See text for details.
[b]After *Goldstein and Jacobsen* [1987]. The fluxes given by these authors are redistributed to the four surface boxes for comparison with our estimates (uncertainty of the estimates is a factor of 2 ∼ 3) [*Goldstein and Jacobsen*, 1987]. All Nd removed in estuaries (70%) are assumed to be released to the solution.
[c]The mineral aerosol flux is estimated from the map of *Duce et al.*, [1991] and the Nd isotopic ratios are estimated from aerosols, sediments and source rocks [*Goldstein et al.*, 1984; *Goldstein and Jacobsen*, 1987, 1988; *Grousset et al.*, 1988, 1992; *McLennan et al.*, 1990; *Nakai et al.*, 1993; *Jones et al.*, 1994].

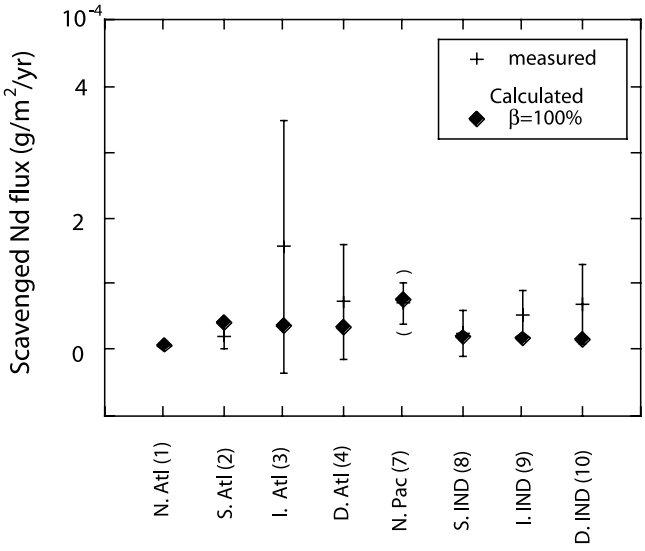

Figure 3. Modeled scavenged Nd fluxes (β = 100%) compared with estimates from field data (Table 2). The large uncertainties in the field data are due to the scattering of data obtained from sites having completely different oceanic conditions. As direct field data are not available for the North Pacific box (>44°N), the flux for this box is derived from data in the Japan Sea (40°N50′) and presented here between blankets. All the calculated fluxes are in agreement with the field data within error.

[25] Finally, we compare the modeled exchanged Nd flux with previous estimates [*Bertram and Elderfield*, 1993]. The exchanged Nd flux is defined as the part of the remineralized Nd flux that is balanced with the authigenic Nd flux formed in the same box. For instance, in the Intermediate INDOPAC (i = 9), the remineralized Nd flux is 4.2×10^9 g/yr and the authigenic Nd flux is 3.7×10^9 g/yr (Table 2). Therefore 3.7×10^9 g/yr of the remineralized Nd flux is balanced with the authigenic Nd flux (an excess of remineralized Nd flux equal to 0.5×10^9 g/yr). Consequently, the exchanged Nd flux in this box is 3.7×10^9 g/yr. In the same manner, the exchanged Nd flux in the whole ocean is estimated at 1.6×10^{10} g/yr. This value corresponds to 40% of the previous estimate (4.2×10^{10} g/yr [*Bertram and Elderfield*, 1993]). These authors applied a seven-box model, using different dissolved Nd concentrations and $\varepsilon_{Nd(0)}$ of the boxes compared with our values. Despite the differences in calculation, there is a satisfactory agreement within the orders of magnitude.

2.4. Sensitivity of Calculated ε_i^{ext}, Nd Residence Time (τ_{Nd}), and Scavenged Nd Fluxes (F_i^{scav}) to Variations in Remineralization Rate (β)

[26] Changes in β influence the Nd influxes (F_i^{ext}) as well as the $\varepsilon_{Nd(0)}$ values (ε_i^{ext}). Let us consider the case of the North Pacific (i = 7). The authigenic particulate Nd flux formed in the box (F_7^p) is remineralized in the Deep INDOPAC (i = 10, Figure 2c). Since ε_7 (−4.0) is higher than ε_{10} (−5.6), this remineralization provides radiogenic Nd to box 10. The magnitude of remineralized Nd flux ($\beta \cdot F_7^p$) is constrained by the balance of $\varepsilon_{Nd(0)}$ and Nd fluxes (equa-tions (3) and (4)). If we decrease β, the value of F_7^p increases to maintain the required $\beta \cdot F_7^p$. The increase in F_7^p requires a higher value of F_7^{ext} to maintain a constant Nd concentration in box 7 (equation (4)). Thus the change in F_7^{ext} produces a modification of ε_i^{ext} (equation (3)). Moreover, the increase in the Nd influx (F_7^{ext}) shortens the oceanic Nd residence time (equation (12)). The sensitivity of the calculated values with respect to β is variable from one box to another, depending upon the required remineralized Nd flux.

[27] The ε_i^{ext} values for the Surface Atlantic (i = 2) and Surface INDOPAC (i = 8) are not sensitive to β: ε_2^{ext} varies only from −11.2 (β = 20%) to −11.4 (β = 100%) and ε_8^{ext} from −4.3 to −4.4 when β ranges from 20% to 100% (Figure 4a). By contrast, ε_i^{ext} for the North Pacific (i = 7) shows a significant variation with β: ε_7^{ext} is stable (−3.9 to −3.4) for β < 60% and increases markedly from −3.4 to +1.1 for β > 60% (Figure 4a).

[28] The calculated τ_{Nd} value is very sensitive to β (Figure 4b). It decreases with β, reaching a value of 30 years at β = 20%. Such a short τ_{Nd} has never been reported for Nd, and is incompatible with the reactivity of this element with marine particles (residence time of Al which is more reactive than Nd, having a residence time is estimated at ∼50 yr). The shortest τ_{Nd} previously reported for Nd is a few hundred of years [*Piepgras and Wasserburg*, 1983]. To obtain this range of τ_{Nd}, β > 60% is required. The relationship between τ_{Nd} and β favors a high remineralization rate.

[29] We compare the calculated scavenged Nd fluxes (F_i^{scav}) with field data using β values of 60 and 80% (Figure 4c). In both cases, F_i^{scav} for the Surface Atlantic and the North Pacific (i = 2, 7) are much higher than the field data. In particular, F_7^{scav} is surprisingly high, corresponding to a value ∼10 times higher than in the other INDOPAC boxes (Figure 4c). There is no geochemical reason for having such a high flux just in the North Pacific box. As the F_i^{scav} values decrease with increasing β, the relationship between F_i^{scav} and β favors a high remineralization rate.

[30] Finally, we can observe the consistency of equations (8a) and (8b) (section 2.1) with respect to varying β. The discrepancy in F_3^p calculated from the two equations decreases with increasing β. It becomes minimal when β =100%. Since both equations should define the same F_3^p, this relationship also supports a high β value.

[31] We use a remineralization rate of 100% in the following discussion, since all the results suggest it is the most appropriate value consistent with the presently available data set.

3. Discussion

3.1. Neodymium Sources to the Ocean

[32] We compare the estimated Nd influxes to the ocean with the sum of riverine and atmospheric inputs. Taking into account that 70% of the dissolved Nd brought in by rivers is removed in estuaries, the net Nd flux from the dissolved river load is 5×10^8 g/yr [*Goldstein and Jacobsen*, 1987]. Using a total mineral aerosol flux of 9.1×10^{14} g/yr [*Duce et al.*, 1991], a Nd concentration in the dust of 20 μg/g [*Goldstein et al.*, 1984; *Grousset et al.*, 1988, 1998] and a soluble Nd proportion of 2% [*Greaves et al.*, 1994], we obtain a net Nd flux from dust of 4×10^8 g/yr. Hence the sum of Nd fluxes from rivers and dust is 9×10^8 g/yr. This

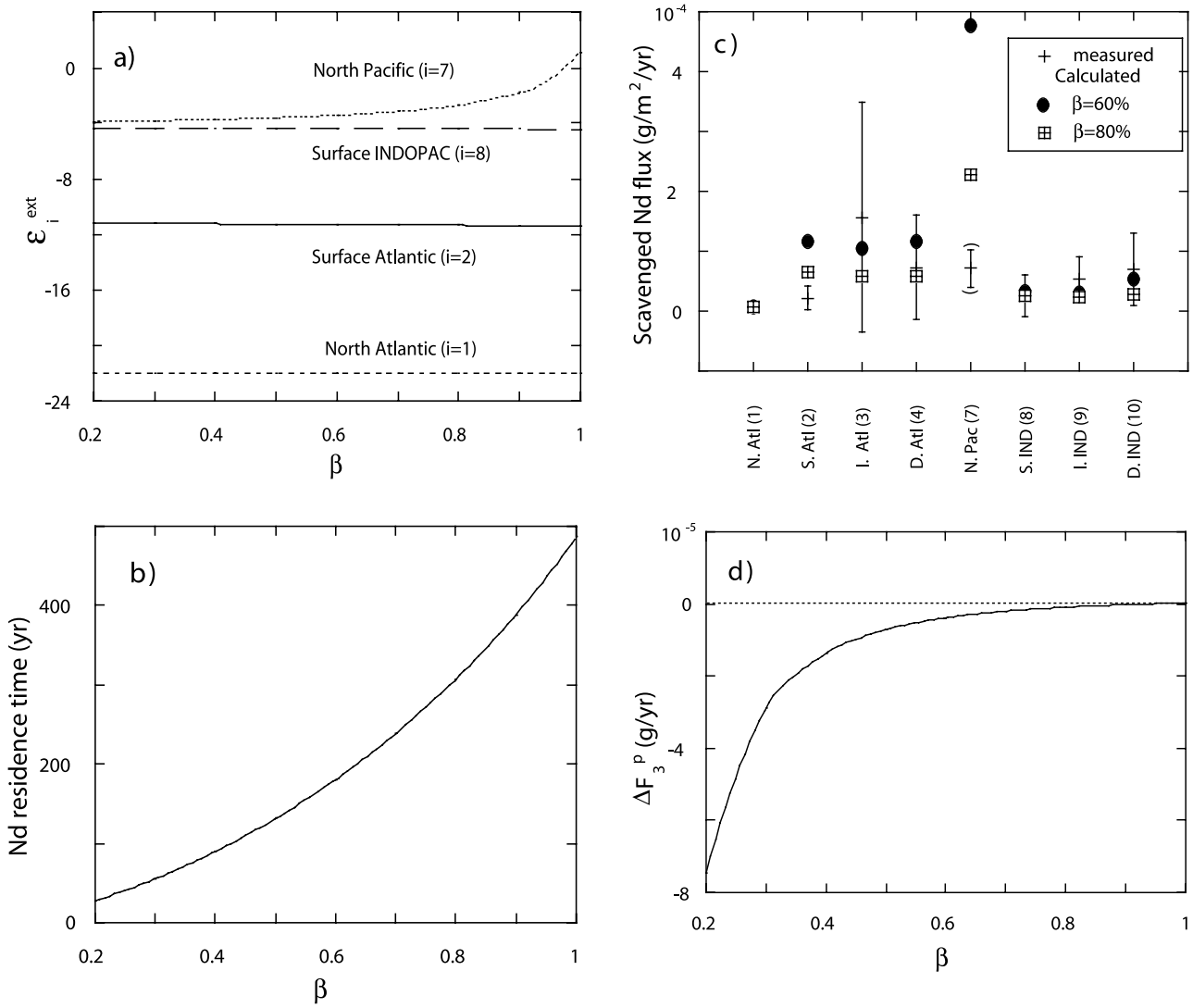

Figure 4. (a) Sensitivities in calculated $\varepsilon_{Nd(0)}$ of external Nd sources (ε_i^{ext}) as a function of β; (b) oceanic Nd residence time as a function of β; (c) modeled scavenged Nd fluxes (β = 60 or 80%) compared with the estimates from field data; and (d) difference in authigenic Nd flux formed in the Intermediate Atlantic box (F_3^p) determined from equations (8a) and (8b) as a function of β.

is about 10 times lower than the calculated total Nd influx, suggesting that other Nd sources may contribute to the oceanic Nd inventory.

[33] Potential Nd sources for the "missing flux" (the difference between the calculated total influx and the sum of dust and river fluxes, 8×10^9 g/yr; Table 3) are as follows: (1) the release of particulate Nd from rivers by contact with seawater [*Spivack and Wasserburg*, 1988; *Sholkovitz*, 1993; *Jones et al.*, 1994; *Byrne and Sholkovitz*, 1996; *von Blanckenburg et al.*, 1996]; (2) a higher dissolution rate (>2%) of Nd from dust [*Henry et al.*, 1994; *Jeandel et al.*, 1995; *Tachikawa et al.*, 1999]; and (3) sediment/seawater interactions at continental margins [*German and Elderfield*, 1990; *Moran and Moore*, 1991; *von Blanckenburg et al.*, 1996; *Jeandel et al.*, 1998; *Amakawa et al.*, 2000; *Lacan and Jeandel*, 2001]. Another potential source is groundwater, which is a significant source for oceanic Ra and Ba [*Moore*, 1997]. However, since no data on Nd isotopic ratios are available, we are unable to quantify the contribution of this source. In the following, we discuss the potential contribution of the first three possible sources only.

3.1.1. Release of Particulate Nd From Rivers by Contact With Seawater

[34] River inputs contribute to both dissolved and particulate Nd in the ocean. Although dissolved riverine Nd is removed from solution in estuaries at 0 $\sim$ 5 psu, a redissolution of removed Nd is observed at higher salinity (5 $\sim$ 35) [*Sholkovitz*, 1993]. As the global river particle flux is huge (1.4×10^{16} g/yr [*Milliman and Meade*, 1983] to 2.3×10^{16} g/yr [*Holeman*, 1968]), the partial dissolution of river particles could be an important Nd source. Assuming that the Nd concentration of river particles is $\sim$30 μg/g [*Goldstein et al.*, 1984], only 1 to 2% of partial Nd dissolution would be sufficient to obtain the missing flux (Table 3). The importance of this source is also suggested by ^{9}Be, another tracer derived from continents [*von Blanckenburg et al.*, 1996].

[35] To evaluate the contribution of "the redissolved Nd", we can assume that all the Nd removed in estuaries goes back into solution. This provides us with an upper limit for the contribution. The total redissolved Nd flux is 1×10^9 g/yr [after *Goldstein and Jacobsen*, 1987], which corresponds to 13% of the total "missing flux" (Table 3). On a regional scale, it represents 75%, 15%, 8% and 7% of the missing flux for the North Atlantic, Surface Atlantic, North Pacific and Surface INDOPAC, respectively.

[36] The $\varepsilon_{Nd(0)}$ of the redissolved Nd flux agrees closely with the value for the missing flux in the Surface Atlantic and Surface INDOPAC boxes (Table 3). By contrast, it differs by +7 and −8 ε units from the $\varepsilon_{Nd(0)}$ value of the missing fluxes in the North Atlantic and North Pacific boxes, respectively. The redissolved Nd flux may not be a prominent Nd source to the North Pacific because of its small contribution (8%) and the discrepancy in $\varepsilon_{Nd(0)}$. We do not totally rule out the possibility of this source to the North Atlantic box because of the uncertainty of ε_1^{ext} related to F_1^p. However, if ε_1^{ext} is correctly estimated, the supplementary Nd source to this box would be characterized by a highly negative $\varepsilon_{Nd(0)}$ of −45, which is not plausible.

[37] River particles consist of several minerals having different $\varepsilon_{Nd(0)}$. Provided that the $\varepsilon_{Nd(0)}$ of soluble river particles is the same as that of river water, we obtain the same $\varepsilon_{Nd(0)}$ distribution as found for redissolved Nd (Table 3). Consequently, river particles could contribute to the Surface Atlantic and Surface INDOPAC boxes. If the $\varepsilon_{Nd(0)}$ of soluble river particles is different from that of river water, river particles may contribute to the budget of Nd in other regions. Volcanic materials (high $\varepsilon_{Nd(0)}$) are suggested to be more soluble than old silicate materials (low $\varepsilon_{Nd(0)}$) [*Albarède and Goldstein*, 1992; *Jones et al.*, 1994]. Therefore this source may contribute to the North Pacific box but probably not to the North Atlantic box.

3.1.2. Higher Dissolution of Nd From Atmospheric Fallout

[38] The proportion of soluble Nd in dust (α) is highly variable ($2 \sim 50\%$) depending on estimation methods. The proportion obtained using Nd isotopes [*Henry et al.*, 1994; *Jeandel et al.*, 1995; *Tachikawa et al.*, 1999] is systematically higher than that based on Nd concentration analysis [*Greaves et al.*, 1994]. The discrepancy is likely related to dissolved/particulate Nd exchanges that can be detected by isotope ratios but not by elemental concentrations. Dust enters the ocean and releases Nd by partial dissolution. If seawater Nd is adsorbed onto dust particles after the dissolution of Nd from the particles, it is impossible to estimate the original proportion of dissolution from the change in Nd concentration (the Nd dissolution is partly canceled by the readsorption). By contrast, $\varepsilon_{Nd(0)}$ may indicate the original dissolution if the $\varepsilon_{Nd(0)}$ of seawater is different from that of the dust. Thus the discrepancy of the estimates may be due to Nd exchange between dust and seawater. Using $\alpha = 30\%$, we obtain a global Nd influx of 6×10^9 g/yr, which almost agrees with the missing flux (Table 3).

[39] We can examine the dust contribution to the missing flux on the basis of $\varepsilon_{Nd(0)}$ assuming that $\alpha = 30\%$. The dust $\varepsilon_{Nd(0)}$ is evaluated from data on aerosols [*Goldstein et al.*, 1984; *Goldstein and Jacobsen*, 1987, 1988; *Grousset et al.*, 1988, 1992], marine sediments [*Grousset et al.*, 1988, 1992; *Nakai et al.*, 1993; *Jones et al.*, 1994] and combining the wind direction with the age of rocks in various source regions [*Goldstein and Jacobsen*, 1987; *McLennan et al.*, 1990]. The dust $\varepsilon_{Nd(0)}$ are approximately −15, −12, −5, and −7 for the North and Surface Atlantic, North Pacific and Surface INDOPAC boxes, respectively (Table 3). The results suggest the lack of nonradiogenic Nd sources to the North Atlantic and radiogenic Nd sources to the North Pacific box (Table 3). In other words, if rivers and dust were the only Nd source for the missing flux, we would be unable to reproduce the regional $\varepsilon_{Nd(0)}$ variation of the sources. This means that additional local Nd sources provide a highly negative $\varepsilon_{Nd(0)}$ to the North Atlantic and a radiogenic Nd component to the North Pacific.

3.1.3. Sediment/Seawater Interaction at the Continental Margins

[40] The $\varepsilon_{Nd(0)}$ of the continental margin is highly variable from region to region: the highest value of the circum-Pacific margin ($\varepsilon_{Nd(0)} = -4.2 \pm 3.8$: [*Jones et al.*, 1994], $\varepsilon_{Nd(0)} = +2 \pm 6$: von Blanckenburg, unpublished compilation) is as high as the estimated $\varepsilon_{Nd(0)}$ of the influx to the North Pacific box. On the other hand, values for Greenland and the Canadian shield ($\varepsilon_{Nd(0)} = -14/-32$ [*Grousset et al.*, 1988]) are as low as the estimated $\varepsilon_{Nd(0)}$ influx to the North Atlantic box. Hence Nd fluxes from the continental margins could generate regional variations of $\varepsilon_{Nd(0)}$ in the influxes.

[41] The release of lithogenic elements from continental margins was originally suggested from Al analysis [*Moran and Moore*, 1991]. Laboratory and field studies (the deep NW Atlantic) suggest that the continuous resuspension and deposition of sediments within the nepheloid layer could promote the release of Al into the overlying water. *Jeandel et al.* [1998] suspected the release of Nd in an area of high hydraulic energy (∼6 Sv) in the Indonesian Strait. Recently, *Amakawa et al.* [2000] showed that remobilization from coastal and shelf sediments may be an important Nd source to the eastern Indian Ocean and its adjacent seas. In the studied area, the riverine dissolved Nd flux appears to be relatively minor. In addition, surface seawater $\varepsilon_{Nd(0)}$ varies over a wide range from −11.4 to −1.3, suggesting a Nd contribution to surface waters from local sources such as old rocks in the Himalayas and from volcanic islands [*Amakawa et al.*, 2000]. The global budget of Be isotopes also suggests that continental margins are of key importance for the ^{9}Be inventory [*von Blanckenburg et al.*, 1996]. The additional flux required for ^{9}Be is $5 \pm 3 \times 10^8$ g/yr [*von Blanckenburg et al.*, 1996], which is about 10 times lower than that for Nd. Interestingly, this difference corresponds to the concentration ratio between these elements in the continental crust (Be and Nd concentrations in the upper continental crust are 3 μg/g and 26 μg/g, respectively [*Taylor and McLennan*, 1985]).

[42] The influence of continental margins on seawater $\varepsilon_{Nd(0)}$ is directly suggested by data from the Mauritanian upwelling region in the NE Atlantic [*Tachikawa et al.*, 1999]. Seawater $\varepsilon_{Nd(0)}$ values off the African continent were analyzed at the E site (∼200 km offshore, 20°N, 18°W) and the M site (∼500 km offshore, 18°N, 21°W). Although the water mass structures are very similar at these sites, the seawater $\varepsilon_{Nd(0)}$ values are different. $\varepsilon_{Nd(0)}$ at the E site (−13.0 to −12.1) is closer to the African continent value (−13 to −12) [*Grousset et al.*, 1992, 1988] than that at the

M site (−12.2 to −10.8). Since this trend is not limited to the surface layer, the partial dissolution of atmospheric dust could not be a major reason for the more negative values at the E site. In fact, the E site is located in the Mauritanian upwelling region where the organic flux is high. The high organic flux produces a reducing environment in the sediments [*Legeleux et al.*, 1994], which could promote a Nd release from coastal sediments during early diagenesis. Fluids containing diagenetic Nd derived from reducing coastal sediments have been observed in other regions [*German and Elderfield*, 1990]. It is noteworthy that the dissolved Nd concentration at the E site is no higher than that at the M site. This may be related to a higher particulate flux at the E site which could remove excess dissolved Nd by scavenging. The influence of margins on seawater $\varepsilon_{Nd(0)}$ is also suggested in the equatorial Pacific [*Lacan and Jeandel*, 2001]. The $\varepsilon_{Nd(0)}$ of the Antarctic Intermediate Water (AAIW) becomes more radiogenic as the AAIW flows along the highly radiogenic Papua New Guinea slope in the Pacific [*Lacan and Jeandel*, 2001]. We do not precisely understand yet how continental margins release terrigenous elements to the ocean. Further studies are required to identify the mechanisms and to quantify the fluxes from this potential source.

3.2. Sensitivity of Deep Water $\varepsilon_{Nd(0)}$ With Nd Influxes: Paleo-Oceanographic Implications

[43] In this section, we examine the sensitivity of deep water Nd concentrations and $\varepsilon_{Nd(0)}$ values by varying the Nd inputs to the ocean. Changes in deep water $\varepsilon_{Nd(0)}$ recorded in ferromanganese crusts and nodules are often interpreted as resulting from modifications in paleoceanic circulation. However, we know that fluxes from the continents to the ocean underwent changes during glacial/interglacial periods. For instance, dust fluxes increased by a factor of 3 to 5 during glacial periods mainly because of an increase in continental aridity [*Rea*, 1994]. Abrasion of the continents by ice sheets could also accelerate the erosion [*Williams et al.*, 1998]. In addition to the changing magnitude of influxes, Nd sources to the ocean might vary with time because of changes in wind direction, aridity of continents, vegetation cover and ice sheets. In this section, we examine whether deep water $\varepsilon_{Nd(0)}$ might vary in response to changing Nd inputs to the ocean, even though oceanic circulation patterns remain unchanged.

[44] We calculate 10 Nd concentrations (C_i) and 10 $\varepsilon_{Nd(0)}$ values (ε_i) at nonsteady state following modifications in the external Nd fluxes (F_i^{ext}) and theirs sources (ε_i^{ext}). Two cases are discussed. In case 1, all the present-day F_i^{ext} are multiplied by a factor of 4, whereas ε_i^{ext} values remain at present-day values. The factor of 4 is chosen to mimic glacial situations with increased dust flux and accumulation rates of lithogenic components in sediments [*Rea*, 1994; *Williams et al.*, 1998]. In case 2, all the F_i^{ext} are taken at the present-day values, whereas all the ε_i^{ext} values are increased by +1 ε-unit ($\Delta\varepsilon_i^{ext} = +1$) to mimic the change in external Nd sources. We use an arbitrary $\Delta\varepsilon_i^{ext} = +1$ to study the response of the deep water $\varepsilon_{Nd(0)}$. The precise estimation of ε_i^{ext} variability with time is beyond the scope of this study.

[45] C_i at nonsteady state is described with 10 differential equations (equation (4), (5), or (6), depending upon the box). These three equations can be applied to any Nd isotope. Using $R_i = {}^{143}Nd/{}^{144}Nd$, equations (4), (5), and (6) can be written as follows:

$$V_i \frac{R_i \cdot C_i}{dt} = \left(R_i^{ext} \cdot F_i^{ext} + \sum_{j \neq i} R_j \cdot F_{j \to i}^{ad} \right) - \left(\sum_{j \neq i} R_i \cdot F_{i \to j}^{ad} + R_i \cdot F_i^p \right) \tag{13}$$

$$V_i \frac{R_i \cdot C_i}{dt} = \left(R_{i-1} \cdot \beta \cdot F_{i-1}^p + \sum_{j \neq i} R_j \cdot F_{j \to i}^{ad} \right) - \left(\sum_{j \neq i} R_i \cdot F_{i \to j}^{ad} + R_i \cdot F_i^p \right) \tag{14}$$

$$V_i \frac{R_i \cdot C_i}{dt} = \left(R_{i-1} \cdot \beta \cdot F_{i-1}^p + \delta_{i,10} \cdot \left(\beta \cdot F_7^p \right). + R_{i-2} \cdot \beta \cdot (1 - \beta) \cdot F_{i-2}^p + \sum_{j \neq i} R_j \cdot F_{j \to i}^{ad} \right) - \left(\sum_{j \neq i} R_i \cdot F_{i \to j}^{ad} + R_i \cdot F_i^p \right) \tag{15}$$

R_i determines an $\varepsilon_{Nd(0)}$ value in box i (ε_i) by fixing $\varepsilon_{Nd(0)}$. The variability in R_i of the 10 boxes is described by 10 differential equations based on equations (13), (14), or (15). Consequently, the Nd inventory at nonsteady state will be determined by 20 differential equations. We apply the following three hypotheses to the modeling. (1) The volume of the 10 boxes (V_i) as well as the advective water fluxes ($F_{i \to j}^{ad,sw}$) are known (Table 1 and Figure 2b) and do not change with time; (2) the authigenic particulate Nd flux (F_i^p) is formed in proportion to the dissolved Nd concentration in box i (C_i), with a constant f_i^p:

$$F_i^p = f_i^p \cdot C_i \tag{16a}$$

$$f_i^p = (F_i^p)_{present} / (Ci)_{present}, \tag{16b}$$

where $(F_i^p)_{present}$ and $(C_i)_{present}$ are present-day F_i^p (Table 2) and present-day C_i (Table 1). f_i^p is assumed not to vary with time; and (3) β is assumed to be 100%.

[46] Under these conditions, 20 differential equations are solved using Matlab. The present-day C_i and ε_i (R_i) are used as an initial condition (Table 1). The model is run for 2000 yr.

[47] We focus here on the Nd variability in the four deep boxes (i = 1, 4, 6 and 10), because the deep water Nd signatures could be recorded in ferromanganese crusts and nodules. The results show that deep water Nd concentrations and $\varepsilon_{Nd(0)}$ change in response to the Nd inputs (Figure 5). In case 1, Nd concentrations in the deep boxes increase by a factor of four, which is proportional to the change in F_i^p (not shown in figure). The deep water $\varepsilon_{Nd(0)}$ values show transitional changes and revert to the initial values (Figure 5a). In case 2 ($\Delta\varepsilon_i^{ext} = +1$), the deep water $\varepsilon_{Nd(0)}$ values increase by +1 ε unit (Figure 5b). When $\Delta\varepsilon_i^{ext}$ is +2, the shift of deep water $\varepsilon_{Nd(0)}$ is also +2 (not shown in figure). Our results suggest that the change in deep water $\varepsilon_{Nd(0)}$ is

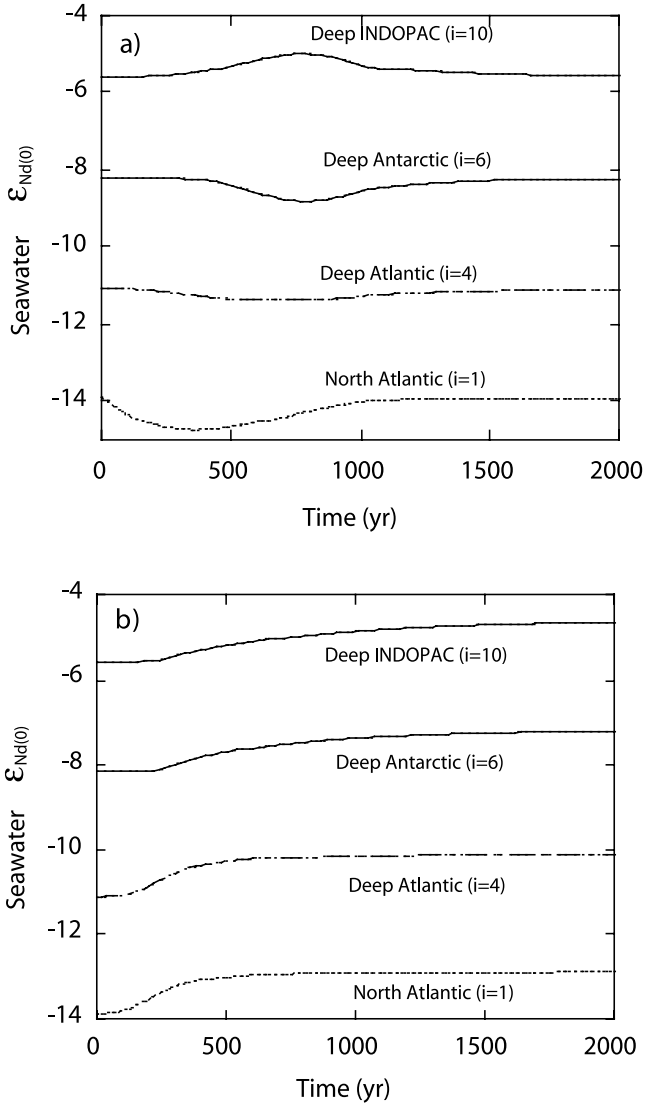

Figure 5. Variability in $\varepsilon_{Nd(0)}$ of the deep waters (boxes 1, 4, 6, and 10) (a) where the Nd influxes (F_i^{ext}) are multiplied by a factor of 4 using the present-day ε_i^{ext} and (b) where the present-day F_i^{ext} values are used with an increased ε_i^{ext} ($\Delta\varepsilon_i^{ext} = +1$). The *x* axis shows the time since modified Nd influxes are introduced to the ocean.

proportional to $\Delta\varepsilon_i^{ext}$. Note that these Nd concentrations and $\varepsilon_{Nd(0)}$ values in deep boxes are obtained under conditions where advective water fluxes remain unchanged.

[48] Up to now, changes in seawater $\varepsilon_{Nd(0)}$ recorded in Fe-Mn nodules, crusts and oxide components of sediments have been generally interpreted as reflecting a variability in paleoceanic circulation. For instance, an increase in $\varepsilon_{Nd(0)}$ in the Antarctic (i = 6) and Indo-Pacific sector (i = 10) could be explained by a decrease in NADW. We show here that a similar $\varepsilon_{Nd(0)}$ shift can be reproduced with no change in NADW (Figure 5b). We also examined the variationbility in deep water $\varepsilon_{Nd(0)}$ using a with β of 70% (not shown in figure). The main trend feature of change is similar to that with β of 100%.

[49] Our results suggest that seawater $\varepsilon_{Nd(0)}$ may vary according to Nd inputs to the ocean as well as changes in water circulation. Since oceanic Nd inputs may vary because of changing conditions of continental erosion, this effect should be considered, in some cases, as accounting for the variability of seawater $\varepsilon_{Nd(0)}$ in the paleo-ocean.

4. Conclusions

[50] The oceanic Nd budget was calculated using a 10-box model (PANDORA) and a compilation of field data. With the currently available data, the best estimates give a Nd flux of 9×10^9 g/yr entering the ocean, which yields an oceanic Nd residence time of ~500 yr. Although neodymium sources to the ocean are highly variable from region to region ($\varepsilon_{Nd(0)}$ from −22 to +1), riverine and atmospheric fluxes cannot explain the variability. Therefore additional Nd sources must be considered. One of the potential Nd sources may be the continental margins.

[51] Using the model calibrated for Nd, we examined the sensitivity of deep water $\varepsilon_{Nd(0)}$ as a function of Nd inputs to the ocean. The deep water $\varepsilon_{Nd(0)}$ value varies in proportion to changes in the $\varepsilon_{Nd(0)}$ of external sources. This implies that shifts in deep water $\varepsilon_{Nd(0)}$ recorded in ferromanganese nodules and crusts do not necessarily reflect changes in oceanic circulation patterns. The deep water $\varepsilon_{Nd(0)}$ shifts could be interpreted in terms of changes in Nd inputs related to continental erosion.

[52] The calibration of our model is essentially based on field data. Although all the available literature data were used to establish the model, more data are required to improve the quality of calibration. In particular, we note that seawater Nd data are scarce in the Antarctic and the North Pacific (north of 44°N). We also require the analysis of sediment-trapped material from the Indian Ocean.

[53] **Acknowledgments.** We thank M. Roy-Barman for fruitful discussions. The initial work of the Nd budget combined with the PANDORA model has greatly benefited from suggestions of W. Broecker. The comments of F. von Blanckenburg, F. Albarède and A. G. Dickson improved the manuscript.

References

Abouchami, W., S. J. G. Galer, and A. Koschinsky, Pb and Nd isotopes in NE Atlantic Fe-Mn crusts: Proxies for trace metal paleosources and paleocean circulation, *Geochim. Cosmochim. Acta*, *63*, 1489–1505, 1999.

Albarède, F., and S. Goldstein, A world map of Nd isotopes in seafloor ferromanganese deposits, *Geology*, *20*, 761–763, 1992.

Albarède, F., S. Goldstein, and D. Dautel, The neodymium isotopic composition of manganese nodules from the Southern and Indian Oceans, the global oceanic neodymium budget, and their bearing on deep ocean circulation, *Geochim. Cosmochim. Acta*, *61*, 1277–1291, 1997.

Amakawa, H., S. D. Alibo, and Y. Nozaki, Nd isotopic composition and REE pattern in the surface waters of the eastern Indian Ocean and its adjacent seas, *Geochim. Cosmochim. Acta*, *64*, 1715–1727, 2000.

Arraes-Mescoff, R., L. Coppola, M. Roy-Barman, M. Souhaut, K. Tachikawa, C. Jeandel, R. Sempere, and C. Yoro, The behavior of Al, Mn, Ba, Sr, REE and Th isotopes during in vitro bacterial degradation of large marine particles, *Mar. Chem.*, *73*, 1–19, 2001.

Bacon, M. P., and R. F. Anderson, Distribution of thorium isotopes between dissolved and particulate forms in the deep sea, *J. Geophys. Res.*, *87*, 2045–2056, 1982.

Bertram, C. J., and H. Elderfield, The geochemical balance of the rare earth elements and Nd isotopes in the oceans, *Geochim. Cosmochim. Acta*, *57*, 1957–1986, 1993.

Broecker, W. S., and T. H. Peng, The role of $CaCO_3$ compensation in the glacial to interglacial atmospheric CO_2 change, *Global Biogeochem. Cycles*, *1*, 15–39, 1987.

Burton, K. W., and D. Vance, Glacial-interglacial variations in the neodymium isotope composition of seawater in the Bay of Bengal recorded

by planktonic foraminifera, *Earth Planet. Sci. Lett.*, *176*, 425–441, 2000.

Burton, K. W., H.-F. Ling, and R. K. O'Nions, Closure of the central American isthmus and its impact on North Atlantic deepwater circulation, *Nature*, *386*, 382–385, 1997.

Byrne, R. H., and E. R. Sholkovitz, Marine chemistry and geochemistry of the lanthanides, in *Handbook on the Physics and Chemistry of Rare Earths*, pp. 527–537, Elsevier Sci., New York, 1996.

De Baar, H. J. W., M. P. Bacon, P. G. Brewer, and K. W. Bruland, Rare-earth elements in the Pacific and in the Atlantic Oceans, *Geochim. Cosmochim. Acta*, *49*, 1953–1959, 1985.

De Baar, H. J., C. R. German, H. Elderfield, and P. Van Gaans, Rare earth element distributions in anoxic waters of the Cariaco Trench, *Geochim. Cosmochim. Acta*, *52*, 1203–1219, 1988.

Duce, R. A., et al., The atmospheric input of trace species to the world ocean, *Global Biogeochem. Cycles*, *5*, 193–259, 1991.

Elderfield, H., The oceanic chemistry of the rare earth elements, *Philos. Trans. R. Soc. London, Ser. A*, *325*, 105–126, 1988.

Elderfield, H., and M. J. Greaves, The rare earth elements in seawater, *Nature*, *296*, 214–219, 1982.

Elderfield, H., R. Upstill-Goddard, and E. R. Sholkovitz, The rare earth elements in rivers, estuaries, and coastal seas and their significance to the composition of ocean waters, *Geochim. Cosmochim. Acta*, *54*, 971–991, 1990.

Fagel, N., L. André, and F. Dehairs, Advective excess Ba transport as shown from sediment and trap geochemical signatures, *Geochim. Cosmochim. Acta*, *63*, 2353–2367, 1999.

Faure, G., *Principles of Isotope Geology*, 200 pp., John Wily, Hoboken, N. J., 1986.

German, C. R., and H. Elderfield, Rare earth elements in Saanich Inlet, British Columbia, a seasonally anoxic basin, *Geochim. Cosmochim. Acta*, *53*, 2561–2571, 1989.

German, C. R., and H. Elderfield, Rare earth elements in the NW Indian Oceans, *Geochim. Cosmochim. Acta*, *54*, 1929–1940, 1990.

German, C. R., T. Masuzawa, M. J. Greaves, H. Elderfield, and J. Edmond, Dissolved rare earth elements in the Southern Ocean: Cerium oxidation and the influence of hydrography, *Geochim. Cosmochim. Acta*, *59*, 1551–1558, 1995.

Goldstein, S. L., and S. B. Jacobsen, The Nd and Sr isotopic systematics of river-water dissolved material: Implications for the sources of Nd and Sr in the seawater, *Chem. Geol.*, *66*, 245–272, 1987.

Goldstein, S. J., and S. B. Jacobsen, Nd and Sr isotopic systematics of river water suspended material: Implications for crustal evolution, *Earth Planet. Sci. Lett.*, *87*, 249–265, 1988.

Goldstein, S. L., R. K. O'Nions, and P. J. Hamilton, A Sm-Nd study of atmospheric dusts and particulate from major river systems, *Earth Planet. Sci. Lett.*, *70*, 221–236, 1984.

Greaves, M. J., M. Rudnicki, and H. Elderfield, Rare earth elements in the Mediterranean Sea and mixing in the Mediterranean outflow, *Earth Planet. Sci. Lett.*, *103*, 169–181, 1991.

Greaves, M. J., P. J. Statham, and H. Elderfield, Rare earth element mobilization from marine atmospheric dust into seawater, *Mar. Chem.*, *46*, 255–260, 1994.

Grousset, F. E., P. E. Biscaye, A. Zindler, J. Prospero, and R. Chester, Neodymium isotopes as tracers in marine sediments and aerosols: North Atlantic, *Earth Planet. Sci. Lett.*, *87*, 367–378, 1988.

Grousset, F., P. E. Biscaye, M. Revel, J.-R. Petit, K. Pye, S. Joussaume, and J. Jouzel, Antarctic (Dome C) ice-core dust at 18 k. y. B.P.: Isotopic constrains on origins, *Earth Planet. Sci. Lett.*, *111*, 175–182, 1992.

Grousset, F. E., M. Parra, A. Bory, P. Martinez, P. Bertrand, G. Shimmield, and R. M. Ellam, Saharan wind regimes traced by the Sr-Nd isotopic compositions of the subtropical Atlantic sediments: Last glacial maximum vs. today, *Quat. Sci. Rev.*, *17*, 395–409, 1998.

Henry, F., C. Jeandel, and J.-F. Minster, Particulate and dissolved Nd in the western Mediterranean Sea: Sources, fates and budget., *Mar. Chem.*, *45*, 283–305, 1994.

Holeman, J. N., Sediment yield of major rivers of the world, *Water Resour. Res.*, *4*, 737–747, 1968.

Jeandel, C., Concentration and isotopic composition of neodymium in the South Atlantic Ocean, *Earth Planet. Sci. Lett.*, *117*, 581–591, 1993.

Jeandel, C., J. K. Bishop, and A. Zindler, Exchange of Nd and its isotopes between seawater small and large particles in the Sargasso Sea, *Geochim. Cosmochim. Acta*, *59*, 535–547, 1995.

Jeandel, C., D. Thouron, and M. Fieux, Concentrations and isotopic compositions of Nd in the eastern Indian Ocean and Indonesian Straits, *Geochim. Cosmochim. Acta*, *62*, 2597–2607, 1998.

Jones, C. E., A. N. Halliday, D. K. Rea, and R. M. Owen, Neodymium isotopic variations in North Pacific modern silicate sediment and the insignificance of detrital REE contribution to seawater, *Earth Planet. Sci. Lett.*, *127*, 55–66, 1994.

Lacan, F., and C. Jeandel, Tracing Papua New Guinea imprint on the central equatorial Pacific Ocean using neodymium isotopic compositions and rare earth elements concentrations, *Earth Planet. Sci. Lett.*, *186*, 497–512, 2001.

Legeleux, F., J. L. Reyss, P. Bonte, and C. Organo, Concomitant enrichments of uranium, molybdenum and arsenic in suboxic continental margin sediments, *Oceanologica Acta*, *17*, 417–429, 1994.

Lerche, D., and Y. Nozaki, Rare earth elements of sinking particulate matter in the Japan Trench, *Earth Planet. Sci. Lett.*, *159*, 71–86, 1998.

Masuzawa, T., and M. Koyama, Settling particles with positive Ce anomalies from the Japan Sea, *Geophys. Res. Lett.*, *16*, 503–506, 1989.

McLennan, S. M., S. R. Taylor, M. T. McCulloch, and J. B. Maynard, Geochemical and Nd-Sr isotopic composition of deep-sea turbidites: Crustal evolution and plate tectonic associations, *Geochim. Cosmochim. Acta*, *54*, 2015–2050, 1990.

Milliman, J. D., and R. H. Meade, World-wide delivery of river sediment to the oceans, *J. Geol.*, *91*, 1–21, 1983.

Moore, W. S., High fluxes of radium and barium from the mouth of the Ganges-Brahmaputra River during low river discharge suggest a large groundwater source, *Earth Planet. Sci. Lett.*, *150*, 141–150, 1997.

Moran, S. B., and R. M. Moore, The potential source of dissolved aluminum from resuspended sediments to the North Atlantic Deep Water, *Geochim. Cosmochim. Acta*, *55*, 2745–2751, 1991.

Murphy, K., and J. Dymond, Rare earth element fluxes and geochemical budget in the eastern equatorial Pacific, *Nature*, *307*, 444–447, 1984.

Nakai, S., A. N. Halliday, and D. K. Rea, Provenance of dust in the Pacific Ocean, *Earth Planet. Sci. Lett.*, *119*, 143–157, 1993.

Nozaki, Y., and J. Zhang, The rare earth elements and yttrium in the coastal/offshore mixing zone of Tokyo Bay waters and Kuroshio, in *Biogeochemical Processes and Ocean Flux in the Western Pacific*, edited by H. Sakai and Y. Nozaki, pp. 171–184, Terra Sci., Tokyo, 1995.

O'Nions, R. K., M. Frank, F. von Blanckenburg, and H.-F. Ling, Secular variation of Nd and Pb-isotopes in ferromanganese crusts from the Atlantic, Indian and Pacific Oceans, *Earth Planet. Sci. Lett.*, *155*, 15–28, 1998.

Piepgras, D. J., and S. B. Jacobsen, The isotopic composition of neodymium in the North Pacific, *Geochim. Cosmochim. Acta*, *52*, 1373–1381, 1988.

Piepgras, D. J., and G. J. Wasserburg, Neodymium isotopic variations in seawater, *Earth Planet. Sci. Lett.*, *50*, 128–138, 1980.

Piepgras, D. J., and G. J. Wasserburg, Isotopic composition of neodymium in waters from the Drake Passage, *Science*, *217*, 207–217, 1982.

Piepgras, D. J., and G. J. Wasserburg, Influence of the Mediterranean outflow on the isotopic composition of neodymium in waters of the North Atlantic, *J. Geophys. Res.*, *88*, 5997–6006, 1983.

Piepgras, D. J., and G. J. Wasserburg, Rare earth element transport in the western North Atlantic inferred from isotopic observations, *Geochim. Cosmochim. Acta*, *51*, 1257–1271, 1987.

Piepgras, D. J., G. J. Wasserburg, and E. G. Dasch, The isotopic composition of Nd in different ocean masses, *Earth Planet. Sci. Lett.*, *45*, 223–236, 1979.

Rea, K. D., The paleoclimatic record provided by eolian deposition in the deep sea: The geologic history of wind, *Rev. Geophys.*, *32*, 159–195, 1994.

Roy-Barman, M., J. H. Chen, and G. J. Wasserburg, ^{230}Th-^{232}Th systematics in the Central Pacific Ocean: The sources and the fates of thorium, *Earth Planet. Sci. Lett.*, *139*, 351–363, 1996.

Rutherg, R. L., S. R. Hemming, and S. L. Goldstein, Reduced North Atlantic Deep Water flux to the glacial Southern Ocean inferred from neodymium isotopic ratios, *Nature*, *405*, 935–938, 2000.

Shimizu, H., K. Tachikawa, A. Masuda, and Y. Nozaki, Cerium and neodymium ratios and REE patterns in seawater from the North Pacific Ocean, *Geochim. Cosmochim. Acta*, *58*, 323–333, 1994.

Sholkovitz, E. R., The geochemistry of rare earth elements in the Amazon River estuary, *Geochim. Cosmochim. Acta*, *57*, 2181–2190, 1993.

Sholkovitz, E. R., and D. L. Schneider, Cerium redox cycles and rare earth elements in the Sargasso Sea, *Geochim. Cosmochim. Acta*, *55*, 2737–2743, 1991.

Spivack, A. J., and G. J. Wasserburg, Neodymium isotopic composition of the Mediterranean outflow and the eastern North Atlantic, *Geochim. Cosmochim. Acta*, *52*, 2762–2773, 1988.

Stordal, M. C., and G. J. Wasserburg, Neodymium isotopic study of Baffin Bay water: Sources of REE from very old terranes, *Earth Planet. Sci. Lett.*, *77*, 259–272, 1986.

Tachikawa, K., Apport des concentrations de Terres Rares et des compositions isotopiques de Néodyme à l'étude de processus dans la colonne d'eau: Cas de l'Atlantique Tropical Nord-Est (sites EUMELI)., Ph.D. thesis, Paul Sabatier, Toulouse, France, 1997.

Tachikawa, K., C. Jeandel, and B. Dupré, Distribution of rare earth elements and neodymium isotopes in settling particulate material of the tropical Atlantic Ocean (EUMELI site), *Deep Sea Res., Part I*, *44*, 1769–1792, 1997.

Tachikawa, K., C. Jeandel, and M. Roy-Barman, A new approach to Nd residence time: The role of atmospheric inputs, *Earth Planet. Sci. Lett.*, *170*, 433–446, 1999.

Taylor, S. R., and S. M. McLennan, *The Continental Crust: Its Composition and Evolution*, 46 pp., Blackwell Sci., Malden, Mass., 1985.

von Blanckenburg, F., P. K. O'Nions, N. S. Belshaw, A. Gibb, and J. R. Hein, Global distribution of beryllium isotopes in deep ocean water as derived from Fe-Mn crusts, *Earth Planet. Sci. Lett*, *141*, 213–226, 1996.

Wasserburg, G. J., S. B. Jacobsen, D. J. De Paolo, M. T. McCulloch, and T. Wen, Precise determination of Sm/Nd ratios, Sm and Nd isotopic abundances in standard solutions, *Geochim. Cosmochim. Acta*, *45*, 2311–2323, 1981.

Westerlund, S., and P. Ohman, Rare earth elements in the Arctic Ocean, *Deep Sea Res., Part A*, *39*, 1613–1626, 1992.

Williams, M., D. Dunkerley, P. De Deckker, P. Kershaw, and J. Chappell, *Quaternary Environments*, 2nd ed., Edward Arnold, London, 1998.

Zhang, J., and Y. Nozaki, Rare earth elements and yttrium in seawater: ICP-MS determinations in the East Caroline, Coral Sea and South Fiji basins of the western south Pacific Ocean, *Geochim. Cosmochim. Acta*, *60*, 4631–4644, 1996.

Zhang, J., H. Amakawa, and Y. Nozaki, The comparative behaviors of Yttrium and Lanthanides in the seawater of the North Pacific, *Geophys. Res. Lett.*, *21*, 2677–2680, 1994.

V. Athias and C. Jeandel, LEGOS, CNES/CNRS/UPS, Observatoire Midi-Pyrénées, 14 av. E. Belin, 31400, Toulouse, France.

K. Tachikawa, CEREGE, Europole de l'Arbois, BP 80, 13545, Aix en Provence, France. (kazuyo@cerege.fr)